Journal of Power Sources 195 (2010) 3207–3214

Contents lists available at ScienceDirect

Journal of Power Sources

journal homepage: www.elsevier.com/locate/jpowsour

Flow uniformity optimization for large size planar solid oxide fuel cells with U-type parallel channel designs

Wuxi Bi, Jiayu Li, Zijing Lin*

Hefei National Laboratory For Physical Sciences at Microscale and Department of Physics, University of Science and Technology of China, Hefei 230026, China

ARTICLE INFO

Article history:
Received 11 October 2009
Received in revised form
16 November 2009
Accepted 25 November 2009
Available online 1 December 2009

Keywords:
Flow uniformity
Planar solid oxide fuel cell
U-type
Gas channel
Optimization

ABSTRACT

The U-type parallel channels for large size planar solid oxide fuel cell (pSOFC) are systematically optimized with the computational fluid dynamics (CFD) method. The CFD calculations are based on realistic 3D gas channel models and typical pSOFC working parameters. The optimized geometric parameters include the height of interconnect ribs, aspect ratios of the inlet-header and outlet-header cross-sections, the sum of inlet- and outlet-header widths and the ratio of the outlet-header width to the inlet-header width (α). Detailed CFD calculations show that a suitable α and a relatively large header width are necessary for the flow uniformity of both air and fuel in large size pSOFCs. In particular, α is demonstrated to be a key parameter for the flow uniformity of large size pSOFCs with U-type parallel channel designs and a proper choice of α is of critical engineering importance. The physical origin for the importance of α on the flow distribution is analyzed.

1. Introduction

An unavoidable development direction of planar solid oxide fuel cells (pSOFCs) is to increase the sizes of active cells in order to efficiently improve the volumetric power densities of working pSOFC stacks. For example, Versa Power Systems and Delphi are reporting manufacturing pSOFCs with active area up to 33 cm × 33 cm [1]. Uniform flow distribution over the active cell area is important for more uniform current generation and reaping the full benefit of a large cell and the stable cell operation. Like the case for high pSOFC stacks [2–5], however, it is nontrivial to achieve flow uniformity for large pSOFC cells. Moreover, in comparison with the flow in a conventional size cell, two new features of the flow in a large size cell may emerge and require additional care. Firstly, the flow in a large size cell may be in the turbulent flow region due to the relatively high flow velocity, while the flow in a conventional size cell is usually laminar [5]. As to be discussed later, this is particularly the case for the air flow and may not be easily treated by simple analytical approximation. Secondly, due to higher flow velocity and longer pathway, the pressure drop for the flow in a large size cell is much larger than that in a conventional size cell. It becomes an important consideration that the overall net pressure drop should be as low as possible to reduce parasitic power needed to drive pump or compressor. Consequently, the flow uniformity for large size pSOFC cells is an important research subject of its own. As the experimental test is expensive, time-consuming and difficult to explore combinations of various design parameters, theoretical approaches are valuable tools for assisting the engineering designs of the gas-flow configurations of large size pSOFC cells.

There have been numerous studies in recent years on the flow distributions inside fuel cell [6–17]. The U-type and Z-type parallel channel designs are the most widely studied flow configurations and the U-type design is favored by many researchers. In most studies, the flow channel system is simplified as a two-dimensional (2D) flow resistance network. Based on the 2D mass and momentum conservation relationships and assuming constant energy loss coefficients for the dividing and combining sections and bends, simple analytical or numerical solutions may be obtained for the flow distributions [6–8]. For example, Maharudrayya et al. [6] obtained an analytical expression for the flow distribution based on 2D mass and momentum equations and the discretization method proposed by Bassiouny and Martin [11] for turbulence flow. Wang [7] introduced the frictional and inertial effects in his 2D model to predict the pressure drop and flow distribution in U-type fuel cells. Although some useful information may be deduced from these 2D models, however, the simplification processes involve numerous approximations that may or may not be valid. Consequently, the 2D results are of limited accuracy at the best and may be misleading sometime.

* Corresponding author. Tel.: +86 551 3606345; fax: +86 551 3606348.
E-mail address: zjlin@ustc.edu.cn (Z. Lin).

0378-7753/$ – see front matter.
doi:10.1016/j.jpowsour.2009.11.127

Nomenclature

A_{fuel}	flow cross-sectional area of fuel inlet
A_{air}	flow cross-sectional area of air inlet
D	hydraulic diameter
F	Faraday's constant (F = 96,485 C mol^{-1})
H_c	channel height
H_{in}	height of the inlet header
H_{out}	height of the outlet header
h_t^{in}	total energy loss due to the friction and local energy loss effects along the inlet header
h_t^{out}	total energy loss due to the friction and local energy loss effects along the outlet header
j	current density
L_{in}	length of the flow cross-sectional area
M_i	molar weight of species i (i = H_2, O_2)
m_i	mass flow rate of the ith channel
m_i'	normalized mass flow rate of the ith channel
$m'_{\min}$	minimal value of the normalized mass flow rates
$\bar{m}$	the average of the channel mass flow rate
P_{drop}	net pressure drop between the flow inlet and outlet
P_i	pressure at the location i (i = A, B, C, D)
Q_{air}	air inlet mass flow rate
Q_{fuel}	fuel inlet mass flow rate
Re	Reynolds number
Re_{air}	Reynolds numbers for air at the inlet
Re_{fuel}	Reynolds numbers for fuel at the inlet
S	effective reaction area
$\vec{u}$	velocity vector
u_i	velocity at the location i (i = A, B, C, D)
U	flow uniformity
V'	gas volumetric flow rate
W_{in}	inlet-header width
W_{out}	outlet-header width
α	ratio of the outlet-header width to the inlet-header width
ζ	inlet-header and outlet-header aspect ratio
ρ	density
ρ_{fuel}	fuel density
ρ_{air}	air density
χ_i	mass fraction of species i in the gas flow (i = H_2, O_2)
η_i	utilization rate of species i (i = H_2, O_2)
η_{pump}	efficiency of the gas pump
τ	stress tensor
μ	fluid viscosity

A more reliable approach to predict the flow distribution is through the computational fluid dynamics (CFD) simulations with realistic 3D flow channel models and reasonable boundary conditions [5,10]. In this work, U-type parallel channel models for large size pSOFCs with realistic geometric parameters were built for both air and fuel flows and full CFD calculations were performed to obtain the details of the flow distributions and pressure drops. Main geometric parameters influencing the channel flow distributions were systematically varied in order to obtain the optimal flow uniformities. The optimized geometric parameters included the height of interconnect ribs, aspect ratios of the inlet-header and outlet-header cross-sections, the sum of inlet- and outlet-header widths and the ratio of the outlet-header width to the inlet-header width. The last parameter is found to be a controlling factor for the flow uniformity and the corresponding physical origin is analyzed.

2. Model description

2.1. U-type gas channels in pSOFC

Fig. 1 shows a U-type flow channel arrangement in a pSOFC cell (the air and fuel channel arrangements are similar and only air channels are explicitly shown). The top component shown is an interconnect plate with parallel channels dug in both sides to distribute the air (fuel) flow across the cell. The corresponding U-type flow model is shown in Fig. 2 and the middle part is the channel group on electrode. The dividing and combining parts of the U-type channel configuration form the inlet header and outlet header, respectively. Without loss of generality, the channel group consists of 50 channels in this study. For naming convenience, the channels are numbered sequentially from the inlet/outlet to the top along the headers. That is, the channel closest to the inlet/outlet is the 1st channel (the bottom channel) and the channel that is furthest away from the inlet/outlet is the 50th cell (the top channel). Fig. 3 shows a 2D cross-section of the U-type flow channel with the corresponding geometrical parameters indicated. The geometric parameters for a standard U-type flow model in this study are shown in Table 1. Unless specified otherwise, the parameters in Table 1 are assumed.

Each geometric variable shown in Table 1 may influence the flow uniformity and pressure drop in some way. Here we limit our discussion to the representative cells with an active area of 200 mm × 200 mm. The width of the channel or rib will also be fixed as their optimization is determined by very different considerations and the used value is reasonable for practical purpose [18–20]. Moreover, based on the results of SOFC stack flow uniformity optimizations, we focus the discussion on the following parameters: the height of the channel on electrode (H_c), the inlet-header and outlet-header aspect ratio ($\zeta = W_{in}/H_{in} = W_{out}/H_{out}$), and the ratio of the outlet-header width to the inlet-header width ($\alpha = W_{out}/W_{in}$).

2.2. Governing equations and flow models for air and fuel

Although the flows in working pSOFC cells are chemical reacting flows and the flow densities and properties change along the channel paths, most flow uniformity studies assume no chemical reactions and the flow is isothermal and incompressible [2–9]. These assumptions are acceptable since chemical reactions and flow property variations occur in all channels on the electrode and a more uniform flow distribution obtained under such assumptions should correspond to a more uniform distribution in practice. To validate the above assertion, some tests were performed using simplified distributions of temperature gradients and electrochemical reactions. For example, the temperature difference between the inlet header and the outlet header was set at 200 K and the temperature gradients and the chemical reactions were assumed to be uniform across the channels. The results for the channel flow rate distributions with the above reacting and non-isothermal flow model were different from the isothermal and non-reacting flow calculations by less than 1%. The differences were insignificant for

Table 1
Geometric parameters for a standard U-type flow model (the reference model) in this study.

Component	Value (mm)
Header's height ($H_{in} = H_{out}$)	3.0
Header's width ($W_{in} = W_{out}$)	8.0
Area of active zone (mm^2)	200.0 × 200.0
Width of channel or rib ($W_c = W_{rib}$)	2.0
Height of fuel channel ($H_c = H_{rib}$)	1.0
Height of air channel ($H_c = H_{rib}$)	1.5

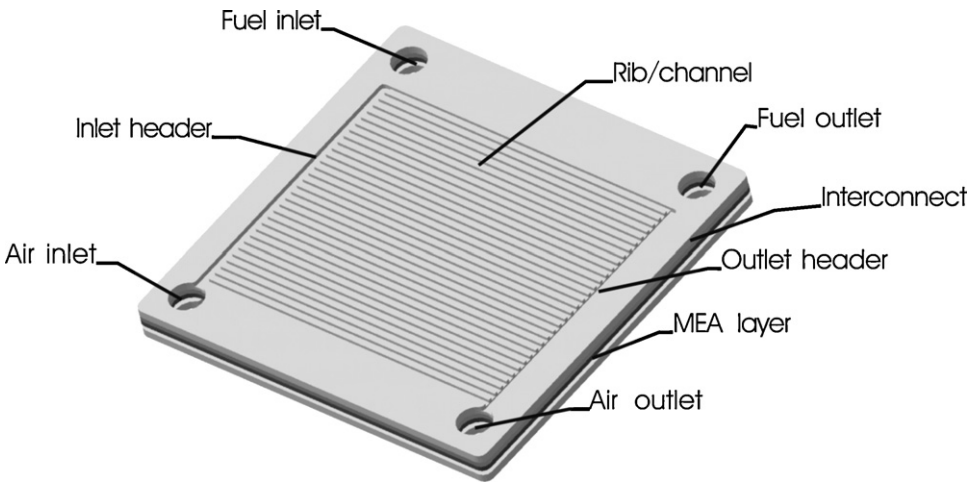

Fig. 1. Planar solid oxide fuel cell with a U-type flow channel design.

the designs of the channel flow distributions. Therefore, this study also adopted the isothermal, non-reacting and incompressible flow assumptions.

The flow governing equations are the continuity equation:

$$\frac{\partial \rho}{\partial t} + \nabla \bullet (\rho \vec{u}) = 0 \tag{1}$$

where $\vec{u}$ is the velocity vector and ρ is the density, and the momentum equation

$$\frac{\partial \rho \vec{u}}{\partial t} + \nabla \bullet (\rho \vec{u} \times \vec{u}) = -\nabla p + \nabla \bullet \tau \tag{2}$$

where τ is the stress tensor.

According to the fluid dynamics, the flow state is characterized by Reynolds number (Re)

$$Re = \frac{\rho u D}{\mu} \tag{3}$$

where u is the average flow velocity, D the hydraulic diameter and μ is the fluid viscosity. For the inlet header with a rectangular cross-sectional area, $D = 2L_{in}W_{in}/(L_{in} + W_{in})$, where L_{in} and W_{in} are respectively the length and width of the flow cross-sectional area. If Re is less than 2100, the flow is laminar. Otherwise, the flow is turbulent.

The mass flow rate at the cell gas channel inlet may be determined by the average current density (j), the effective reaction area (S), the fuel/oxidant utilization rate (η) and the mass fraction of the effective component in the gas flow (χ).

Considering a representative fuel consisting of 65% hydrogen and 35% water by mass fraction, the inlet fuel mass flow rate may be written as

$$Q_{fuel} = \rho_{fuel} A_{fuel} u_{fuel} = \frac{jSM_{H_2}}{2F\eta_{H_2}\chi_{H_2}} \tag{4}$$

where M_{H_2} is the molar weight of hydrogen ($M_{H_2} = 2.0\,\mathrm{g\,mol^{-1}}$), F the Faraday constant ($F = 96{,}485\,\mathrm{C\,mol^{-1}}$), η_{H_2} ($= 0.85$) the overall hydrogen utilization rate, χ_{H_2} ($= 0.65$) the mass fraction of hydrogen in the inlet fuel flow. In this study, the average current density, j, is set at $0.7\,\mathrm{A\,cm^{-2}}$, and the effective reaction area, S, is $400\,\mathrm{cm^2}$.

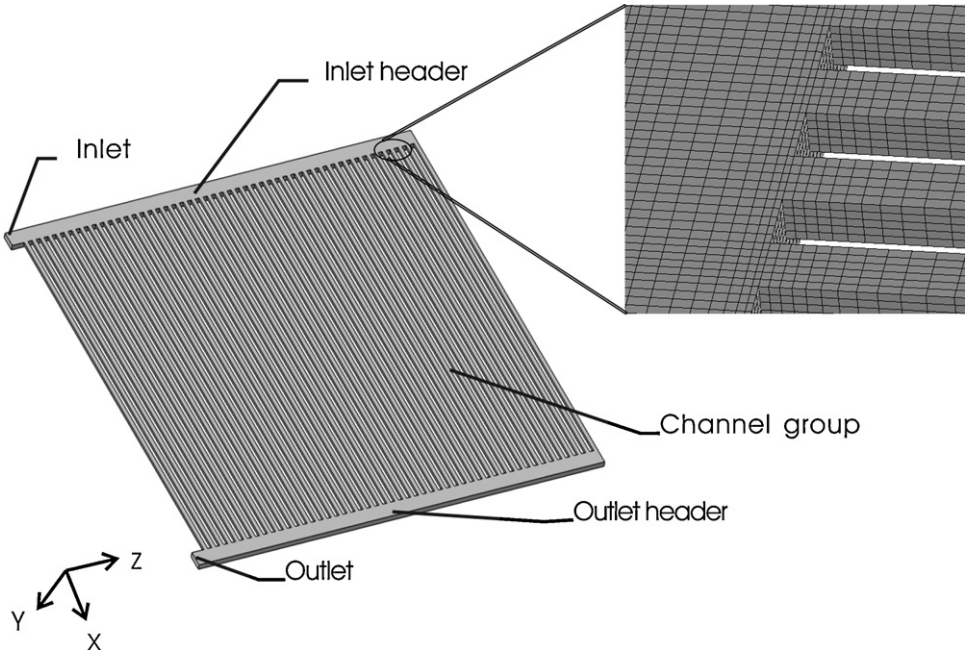

Fig. 2. A U-type flow model with 50 channels in the channel group and a grid subset for the model.

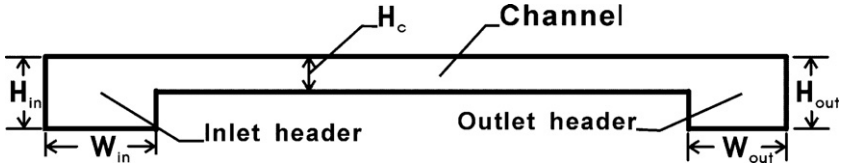

Fig. 3. A 2D cross-sectional view of a U-type flow channel.

Similarly, the inlet air mass flow rate may be expressed as

$$Q_{air} = \rho_{air} A_{air} u_{air} = \frac{jSM_{O_2}}{4F\eta_{O_2}\chi_{O_2}} \quad (5)$$

where η_{O_2} (=0.15), χ_{O_2} (=0.21) and M_{O_2} (=32 g mol^{-1}) are the oxygen usage rate, oxygen mass fraction in air and the molar weight of oxygen, respectively.

Based on Eqs. (3)–(5), the Reynolds numbers for fuel and air at the inlets may be written as

$$Re_{fuel} = \frac{jSM_{H_2}}{F\eta_{H_2}\chi_{H_2}\mu_{fuel}(L_{in} + W_{in})} \quad (6)$$

$$Re_{air} = \frac{jSM_{O_2}}{2F\eta_{O_2}\chi_{O_2}\mu_{air}(L_{in} + W_{in})} \quad (7)$$

The flow viscosity may vary with the temperature and components and was evaluated with the Sutherland's law [21]. At the working temperature of 1073 K, the fuel and air viscosities are 3.01×10^{-5} and 4.16×10^{-5} kg m^{-1} s^{-1}, respectively.

According to the parameters in Table 1 and those given above, Re_{fuel} is found to be around 300, and Re_{air} is about 6000, indicting that the fuel flow is well in the laminar flow region, while the air flow as a whole is in the turbulent region. Therefore, the CFD calculations for the air flow in large size pSOFC must adopt the turbulence models, a situation very different from that for a conventional size pSOFC ($S \approx 100$ cm^2, $Re_{air} \approx 1500$) where a laminar flow model may be appropriate.

2.3. Measure of flow uniformity (U)

There are different definitions of flow uniformity in literatures. Similar to the definition proposed for the stack flow uniformity in a previous study [5], the flow uniformity, U, is defined here as the minimal value of the normalized mass flow rates (m'_{min}) of all channels in the channel group:

$$U = m'_{min} \quad (8)$$

Here the normalized mass flow rate is defined as

$$m'_i = \frac{m_i}{\bar{m}} \quad (i = 1, 2, \ldots, 50) \quad (9)$$

where m_i is the mass flow rate of the ith channel and $\bar{m}$ is the average of m_i. Clearly, $0 \le U \le 1$ and a higher value of U indicates a more uniform flow distribution with $U = 1$ corresponds to the perfectly uniform flow where all channels receive the same amount of flow. Notice that the flow uniformity requirement for the cell channels is less stringent than that for the stack flow. The cells in a pSOFC stack are connected in series to produce the current and the possible stack power output is limited by the cell receiving the least flow, while the channels in a cell are connected in parallel and the effect of non-uniform flow is less severe. However, flow non-uniformity does mean that some channels are less effective and reduce the benefit of a large cell. Moreover, flow non-uniformity may also have other undesirable consequences such as inducing local hot/cold spots and high thermal stress.

2.4. Pressure drop and the electric power loss

Denoting the net pressure drop between the flow inlet and outlet as P_{drop}, the electrical power required to drive the gas pump or compressor may be estimated as $P_{drop}V'/\eta_{pump}$, where V' is the gas volumetric flow rate and η_{pump} is the efficiency of the gas pump. V' may be calculated as the mass flow rate (Eq. (4) or (5)) divided by the gas density at the working condition. For the reference model working at 1073 K and 1 atm and assuming the cell output voltage of 0.7 V and $\eta_{pump} = 0.85$, it is easy to know that for every P_{drop} of 1000 Pa, about 1.2% and 0.1% of the electric power produced by the pSOFC cell will be consumed by the air and fuel pumps, respectively. Clearly, even though a uniform flow distribution may be obtained by ensuring that the pressure-change in inlet/outlet headers is much lower than that in the gas channels, excessively large P_{drop} should be avoided in order for the pSOFC technology to be competitive in overall system efficiency. The role of P_{drop} for the air flow is particularly important for the system efficiency. Therefore, high flow uniformity with relatively low net pressure drop for air should be a goal of engineering design.

2.5. CFD settings and solutions

2.5.1. Grid generation

Commercial software ANSYS® ICEM CFD 11.0 was used in the grid generation. The reference model was divided into a fine grid of approximately 420,000 hexahedral elements. For both the air and fuel flow models, the average grid dimensions for the inlet and outlet headers were 0.60 mm × 0.20 mm × 0.40 mm in X, Y and Z directions (see Fig. 2 for the definition of the coordinate axes). The size of the mesh cells was kept unchanged as far as possible for models other than the reference one and the number of the grid cells changed proportionally with the model geometry dimension. Each of the flow channels was simulated by five cells across each dimension (Y and Z directions) regardless of the geometry dimension variation of the flow channels. The average grid dimension in the X direction was 2.50 mm for the flow channels in all models. The mesh resolution for a subset of the model is illustrated in Fig. 2. The flow fields around headers and channel junctions are portrayed with grids finer than the above average in order to describe the flow field better. To test the model grid independence, several calculations have been carried out and the grid model is verified to be sufficiently fine. For example, the maximum deviation for the standard model is found to be only 0.5% (2%) for the air (fuel) flow uniformity between the results using the above grid and a similar but coarser grid composed of approximately 97,000 hexahedral elements.

2.5.2. Boundary conditions

Mass flow rate inlet boundary and pressure outlet boundary conditions were adopted for the flow models. The mass flow rate for fuel and air are determined by Eqs. (4) and (5). The reference static pressure was 1 atm and the outlet pressure profile blend factor was set at 0.05. Adiabatic, no-slip walls and the scalar wall function were used to treat the wall boundaries [22].

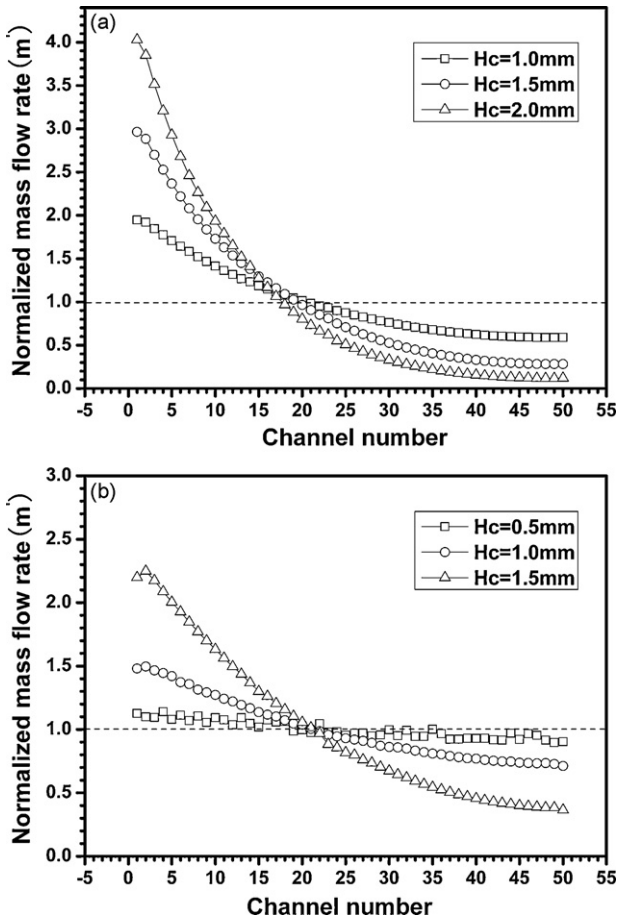

Fig. 4. The effect of the channel height (H_c) on the flow uniformity of the reference model: (a) air flow, (b) fuel flow. The air and fuel uniformities increase with the decrease of H_c.

2.5.3. Solutions

Commercial software, ANSYS® CFX 11.0, was used in the CFD calculations. According to the above discussion in Section 2.2, the standard k–ε turbulence flow model for the air flow system and laminar flow model for the fuel flow system were used in the CFD settings. The standard k–ε turbulence flow model is widely used, as it offers good compromise between numerical effort and computational accuracy. The value of k and ε at the inlet were assigned to a 5% turbulence intensity level. Changing the turbulence intensity level from 1% to 10% only resulted in a change of the air flow uniformity by less than 1% for the reference model. The convergence target RMS was set at 10^{-5}, which was known to provide highly convergent results.

3. Results and discussions

3.1. The effects of H_c on the gas distribution

Fig. 4 shows the effects of the channel height (H_c) on the air and fuel distributions. Air flow uniformity increases from 0.12 to 0.59 when H_c decreases from 2.0 to 1.0 mm. Meanwhile, P_{drop} increases from 3118 to 3642 Pa in the process. Similarly, the fuel uniformity increases from 0.39 to 0.91 when H_c is decreased from 1.5 to 0.5 mm, while P_{drop} is changed from 1348 to 3434 Pa. The effect of H_c on the flow uniformity is easily understandable. Reducing H_c increases the difficulty of gas flowing through the small channels and a larger pressure drop is required for passing through the same amount of flow. Consequently, the pressure drops in inlet header and outlet header become relatively small in comparison with that in the channels, resulting in the improved uniformity of the channel flows. As a note in passing, the pressure drop results may be understood by assuming P_{drop} is approximately proportional to the flow velocity of the channel receiving the most flow. For example for the air flow, the maximum flow velocity, which is proportional to the maximal normalized mass flow rate multiplied by the average flow velocity (the latter is inversely proportional to the channel height), remains roughly unchanged for different H_c, as may be inferred from Fig. 4a. Consequently, P_{drop} for the air flow is roughly the same for different H_c.

Notice, however, according to the discussion in Section 2.4, the air pressure drop of over 3000 Pa translates to a significant loss of about 4% of the electric power produced and is highly undesirable. Therefore, reducing H_c is not a good design option even though it is helpful for improving the flow uniformity.

3.2. The effects of ζ on the flow distribution

In this study, the cross-sectional area of either the inlet or outlet header, $W_{in} \times H_{in}$ (=$W_{out} \times H_{out}$), were fixed at 24 mm^2 and the header's aspect ratio ζ ($\zeta = W/H$) was varied as 12 mm/2 mm = 6.00, 8 mm/3 mm = 2.67 and 6 mm/4 mm = 1.50. As shown in Fig. 5, with ζ decreased from 6.00 to 1.50, the air and fuel uniformities increase from 0.24 to 0.31 and from 0.55 to 0.79, respectively. Meanwhile, P_{drop} for air and fuel decrease from 3517 to 3180 Pa and from 3080 to 1866 Pa, respectively. It appears that ζ affects the flow uniformity and the pressure drop more for fuel than for air. This is due to that the fuel flow is laminar and the energy loss is dominated by the

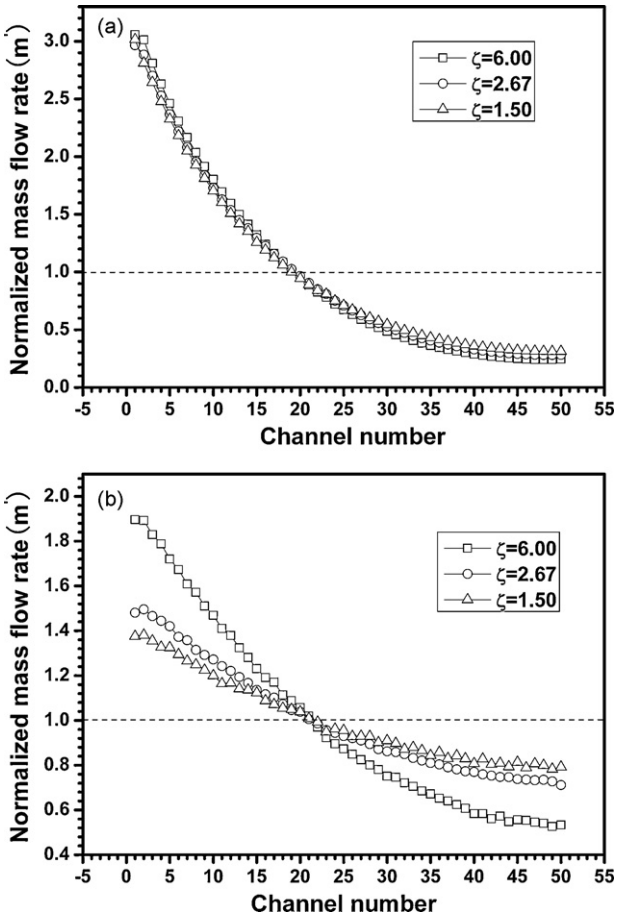

Fig. 5. The effects of ζ ($\zeta = W/H$) on the gas distribution: (a) air flow, (b) fuel flow.

friction effect that is sensitive to the aspect ratio. The air flow, however, is turbulent and the energy loss is dominated by the kinetic term that is not directly related to the aspect ratio. The frictional energy loss is only of secondary importance for the air flow. Consequently, the effect of the aspect ratio on the flow uniformity is more notable for the fuel flow than for the air flow.

It is clear that a smaller ζ is beneficial for both air and fuel flow distributions. This is understandable based on the approximate laminar flow theory: a smaller ζ means a lower flow friction and smaller pressure drop along the headers and consequently the pressure drop in the headers becomes relatively small in comparison with that in the channels, resulting in the improved uniformity of the channel flows. It is advisable to use a head with small ζ in order to improve the fuel uniformity. However, it is difficult to improve the air flow uniformity and reduce the air pressure drop to the desired level by reducing ζ and alternative design parameter should be sought.

3.3. The effects of α on the flow uniformity

α is defined as the ratio of the outlet-header width to the inlet-header width, W_{out}/W_{in}. The effects of α on the flow uniformity were examined with a constant $W_{in} + W_{out}$ so that the cells with different α may have the same volumetric power density design.

3.3.1. Air flow distribution

The cases for $W_{in} + W_{out}$ = 12, 16, 20 and 24 mm were examined. In each case, α was varied between 1.00 and 3.00. Some representative results are shown in Fig. 6. As may be seen from Fig. 6, suitable choice of α may significantly improve the air flow uniformity. It is interesting to note that the four cases of $W_{in} + W_{out}$ = 12, 16, 20 and 24 mm share the same optimal α (α = 2.2) for achieving the highest flow uniformity. The highest flow uniformities obtained were respectively 0.86, 0.94, 0.95 and 0.95 with the corresponding P_{drop} of 6357, 3687, 2451 and 1774 Pa. Compared to all the results discussed so far with α = 1, the air flow uniformity is greatly improved with the optimized α (=2.2) and α is a key design parameter for the air flow uniformity. In addition, it is clear that a larger value of $W_{in} + W_{out}$ is helpful for achieving higher flow uniformity and lower overall pressure drop. Even though the effect of using $W_{in} + W_{out}$ larger than 16 mm on the optimal flow uniformity is quite limited, it is still quite helpful for reducing the pressure drop. A value of $W_{in} + W_{out}$ larger than 24 mm is recommended to further reduce the air pressure drop.

3.3.2. Fuel flow distribution

The effects of α on the fuel flow uniformity were similarly tested and the representative results are shown in Fig. 7. The highest flow uniformities for $W_{in} + W_{out}$ = 12, 16, 20 and 24 mm were found with the same α, α = 1, and were respectively 0.57, 0.71, 0.78 and 0.83 with the corresponding P_{drop} of 2580, 2189, 1943 and 1849 Pa. Similar to the findings for the air flow, a larger value of $W_{in} + W_{out}$ is helpful for achieving higher fuel flow uniformity as well as lower pressure drop. A value of $W_{in} + W_{out}$ larger than 24 mm is also recommended to further improve the flow uniformity. However, the effects of α on the fuel flow appear to be characteristically different from that on the air flow. For all the cases studied, the optimal α for the fuel flow is α = 1 and the flow uniformity decreases gradually with the increase of α. The underlying mechanism will be analyzed later.

3.4. The mechanism for the role of α on the flow distribution

The above results have shown that the ratio of the outlet-header width to the inlet-header width, α, is a critically important design parameter for the air flow uniformity with low pressure drop. Analyzing the underlying mechanism is not only helpful for understanding the modeling results, but also useful for providing a general guiding principle to the broad pSOFC community.

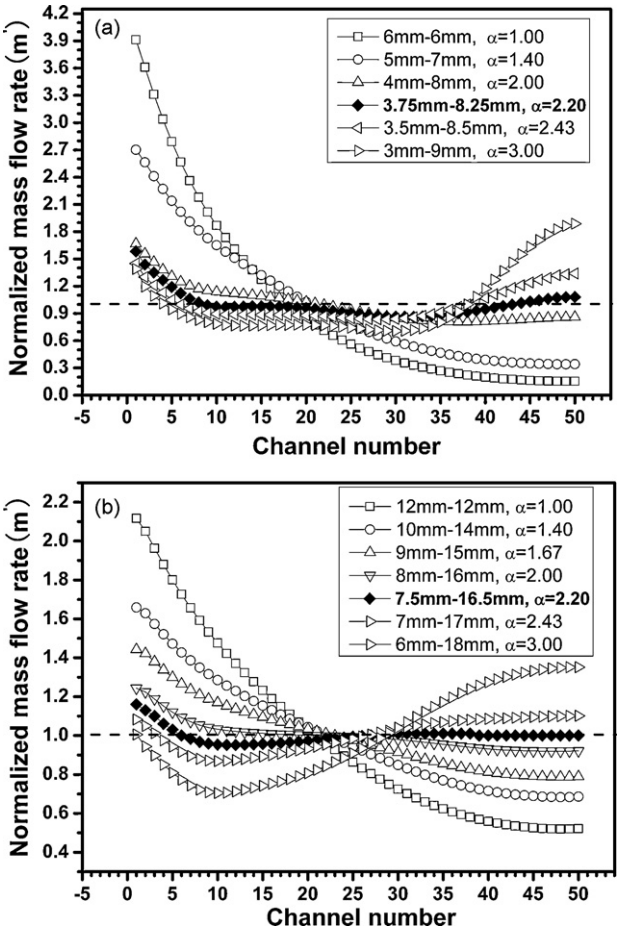

Fig. 6. Dependence of air flow distributions on α: (a) $W_{in} + W_{out}$ = 12 mm, (b) $W_{in} + W_{out}$ = 24 mm.

The basic physics of the 3D U-type channel flows (Fig. 2) may be represented by the simplified 2D model shown in Fig. 8. The energy conservation relationship along the inlet header (A–B) and the outlet header (C–D) may be written as [23]:

$$P_A + \frac{1}{2}\rho u_A^2 = P_B + \frac{1}{2}\rho u_B^2 + h_t^{in} \tag{10}$$

$$P_C + \frac{1}{2}\rho u_C^2 = P_D + \frac{1}{2}\rho u_D^2 + h_t^{out} \tag{11}$$

where h_t^{in} and h_t^{out} are the total energy loss due to the friction and other local energy loss effects along the inlet header and the outlet header, respectively. P_i (u_i) is the pressure (velocity) at the location i (i = A, B, C, D).

Due to the flow mass conservation, the average velocities in the inlet header and the outlet header may be expressed as

$$u_A = \alpha u_D, \quad u_B = \alpha u_C \tag{12}$$

Combining Eqs. (10)–(12) gives

$$(P_A - P_D) - (P_B - P_C) = h_t^{in} + h_t^{out} - \frac{1}{2}\rho(\alpha^2 - 1)(u_D^2 - u_C^2) \tag{13}$$

For conventional design with the same width for the inlet header and outlet header (α = 1), we always have $(P_A - P_D) > (P_B - P_C)$ since the total energy loss along the headers is always positive. That is, the pressure difference between A and D is always larger than that

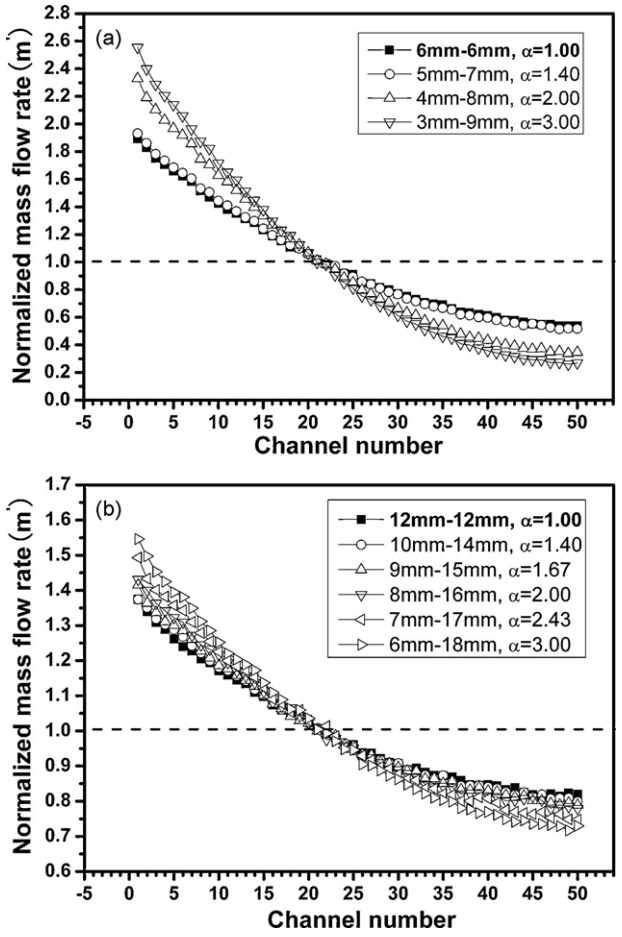

Fig. 7. Dependence of fuel flow distributions on α: (a) $W_{in} + W_{out} = 12$ mm, (b) $W_{in} + W_{out} = 24$ mm.

between B and C. As the mass flow rate for a given channel is roughly proportional to the pressure drop along the channel, the mass flow rate for the first channel A–D is always larger than for the last channel B–C. This analysis is fully supported by the numerical results shown in Figs. 4–7.

If a uniform flow were possible, it would require $(P_A - P_D) \approx (P_B - P_C)$. According to Eq. (13), this can only be achieved with $\alpha > 1$ because $(u_D^2 - u_C^2)$ is always positive. Further increasing the value of α beyond a balancing point may cause

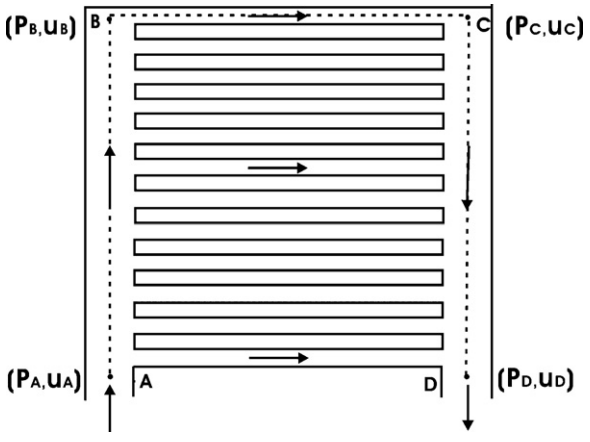

Fig. 8. A simplified 2D model of the 3D air or fuel flow in a pSOFC cell.

$(1/2)\rho(\alpha^2 - 1)(u_D^2 - u_C^2) > h_t^{in} + h_t^{out}$, or $(P_A - P_D) < (P_B - P_C)$. In that case, the last channel may receive more flow than the first channel. This analysis is also fully supported by the numerical results shown in Fig. 6. Moreover, the local energy loss is proportional to the square of the flow velocity [24,25] and the total energy loss along the headers (h_t^{in} and h_t^{out}) is dominated by the local energy loss when the flow velocity is high. That is, both $h_t^{in} + h_t^{out}$ and $(u_D^2 - u_C^2)$ are roughly inversely proportional to the square of the inlet-header width. Therefore, cells with different $W_{in} + W_{out}$ are seen to have essentially the same optimal α_0 that gives $(1/2)\rho(\alpha_0^2 - 1)(u_D^2 - u_C^2) \approx h_t^{in} + h_t^{out}$, as illustrated in Fig. 6.

When the flow velocity is small like the case for the typical fuel flow, the frictional energy loss can be a major or dominant component of the total energy loss. In such cases, only very large α may achieve the balance $(1/2)\rho(\alpha^2 - 1)(u_D^2 - u_C^2) \approx h_t^{in} + h_t^{out}$. For practical α, $(1/2)\rho(\alpha^2 - 1)(u_D^2 - u_C^2)$ may increase slower than $h_t^{in} + h_t^{out}$ with the increase of α. As a result, the difference between $(P_A - P_D)$ and $(P_B - P_C)$ may increase with the increase of α, as observed in Fig. 7 for the fuel flow. Fortunately, the fuel flow uniformity is already reasonably high for the conventional design of $W_{in} = W_{out} = 12$ mm. Adjusting the head aspect ratio may further increase the flow uniformity (Fig. 5b). Moreover, the fuel flow may tolerate a relatively high pressure drop (Section 2.4). It is easy to further improve the flow uniformity by moderately reducing the fuel channel height.

4. Summary

We have constructed realistic 3D U-type flow field models for large size pSOFCs. The effects of the channel height, the header aspect ratio and the header width ratio (α) on the flow uniformity and the total pressure drop have been systematically examined with the CFD method. α is found to be a key parameter for the air flow uniformity and the underlying mechanism is clearly explained by a simplified 2D model.

Acknowledgments

We gratefully acknowledge the financial support of the Knowledge Innovation Program and the Key Program of the Chinese Academy of Sciences (KJCX1.YW.07), the National High-tech R&D Program of China (2007AA05Z156) and the National Science Foundation of China (10574114).

References

[1] B. Borglum, in: 10th Annual SECA Workshop, Pittsburgh, PA, July 15, 2009.
[2] R.J. Boersma, N.M. Sammes, J. Power Sources 63 (1996) 215–219.
[3] R.J. Boersma, N.M. Sammes, J. Power Sources 66 (1997) 41–45.
[4] K. Joon-Ho, S. Hai-Kyung, G.L. Choong, Y. Young-Sung, C.L. Hee, J. Power Sources 115 (2003) 54–65.
[5] W.X. Bi, D.F. Chen, Z.J. Lin, Int. J. Hydrogen Energy 34 (2009) 3873–3884.
[6] S. Maharudrayya, S. Jayanti, A.P. Deshpande, J. Power Sources 144 (2005) 94–106.
[7] J.Y. Wang, Int. J. Hydrogen Energy 33 (2008) 6339–6350.
[8] W.L. Huang, Q.S. Zhu, J. Power Sources 178 (2008) 353–362.
[9] R.J. Kee, P. Korada, K. Walters, M. Pavol, J. Power Sources 109 (2002) 148–159.
[10] M.S. Hyun, S.K. Kim, D. Jung, B. Lee, D. Peck, T.J. Kim, Y.G. Shul, J. Power Sources 157 (2006) 875–885.
[11] M.K. Bassiouny, H. Martin, Chem. Eng. Sci. 39 (1984) 693–700.
[12] C.M. Huang, S.S. Shy, C.H. Lee, J. Power Sources 83 (2008) 205–213.
[13] C.H. Cheng, H.H. Lin, J. Power Sources 194 (2009) 349–359.
[14] W. Zhang, P. Hu, X. Lai, L. Peng, J. Power Sources 194 (2009) 931–940.
[15] J.H. Jang, W.M. Yan, H.Y. Li, W.C. Tsai, Int. J. Hydrogen Energy 33 (2008) 156–164.
[16] G. Hu, J. Fan, S. Chen, Y. Liu, K. Cen, J. Power Sources 136 (2004) 1–9.
[17] D.H. Jeon, S. Greenway, S. Shimpalee, J.W. Van Zee, Int. J. Hydrogen Energy 33 (2008) 1052–1066.

[18] S.X. Liu, W. Kong, Z.J. Lin, J. Power Sources 194 (2009) 854–863.
[19] S.X. Liu, C. Song, Z.J. Lin, J. Power Sources 183 (2008) 214–225.
[20] Z.J. Lin, J.W. Stevenson, M.A. Khaleel, J. Power Sources 117 (2003) 92–97.
[21] R. O'Hayre, S.W. Cha, W. Colella, F.B. Prinz, Fuel Cell Fundamentals, John Wiley & Sons Inc., 2005, pp. 151–154.
[22] ANSYS CFX 11.0 help document, Ansys Inc., 2006.
[23] K. Oka, H. Ito, Trans. ASME 127 (2005) 110–116.
[24] M. Serre, A.J. Odgaard, R.A. Elder, J. Hydraul. Eng. 120 (1994) 808–830.
[25] W.H. Hager, in: Proceedings of the Institution of Mechanical Engineers, 1984, pp. 63–69.